

Antibonding Ground States in InAs Quantum-Dot Molecules

M. F. Doty,^{1,*} J. I. Climente,² M. Korkusinski,³ M. Scheibner,¹ A. S. Bracker,¹ P. Hawrylak,³ and D. Gammon¹

¹Naval Research Laboratory, Washington, D.C. 20375, USA

²CNR-INFM National Center on nanoStructures and bioSystems at Surfaces (S3), Via Campi 213/A, 41100 Modena, Italy

³Institute for Microstructural Sciences, National Research Council of Canada, Ottawa, Canada K1A 0R6

(Received 19 September 2008; published 28 January 2009)

Coherent tunneling between two InAs quantum dots forms delocalized molecular states. Using magnetophotoluminescence spectroscopy we show that when holes tunnel through a thin barrier, the lowest energy molecular state has bonding orbital character. However, as the thickness of the barrier increases, the molecular ground state changes character from a bonding orbital to an antibonding orbital, confirming recent theoretical predictions. We explain how the spin-orbit interaction causes this counterintuitive reversal by using a four-band $k \cdot p$ model and atomistic calculations that account for strain.

DOI: 10.1103/PhysRevLett.102.047401

PACS numbers: 78.67.Hc, 78.20.Ls, 78.47.-p, 78.55.Cr

Quantum dots have confined energy levels analogous to ordinary atoms. Two quantum dots in close proximity can be viewed as an artificial diatomic molecule when coherent tunnel coupling leads to the formation of delocalized states. The properties of such quantum-dot molecules (QDMs) have been the focus of much research because of potential applications in novel optoelectronic devices or quantum information processing. In analogy with natural diatomic molecules, one expects the lowest energy delocalized molecular state to have bonding orbital character. However, recent theoretical studies have predicted that the molecular ground state for a hole in an InAs QDM can have antibonding character [1–3]. If verified by experiment, an antibonding molecular ground state would provide a striking example of a novel property of artificial atoms that cannot simply be explained as a rescaled version of the physics of real atoms.

In this Letter we present the first experimental observation of an antibonding molecular ground state. We find that the molecular ground state changes character from a bonding orbital to an antibonding orbital as the thickness of the barrier separating the two coupled quantum dots is increased. Using a four-band $k \cdot p$ model validated by atomistic calculations, we explain how this counterintuitive result arises from the spin-orbit (SO) interaction.

We use magneto-optical spectroscopy to study QDMs composed of two vertically stacked InAs/GaAs quantum dots separated by a GaAs barrier. The two dots have different size, composition, and strain, and therefore different confined energy levels. As a result, the electron and hole tend to localize in individual dots, as depicted in the left-hand insets of Fig. 1. Delocalized molecular states are formed by coherent tunneling [4] when an electric field tunes the relative energies of confined states in the two dots through resonance [5–7]. Either electron or hole tunneling can be induced [8], but in this work we focus only on hole tunneling. Because of the large inhomogeneous distribution of parameters in ensembles of QDMs, all spectroscopy is performed on single QDMs.

Figure 1 shows the anticrossing of the neutral exciton (X^0) that results from coherent tunneling of a single hole through a thin (2 nm) barrier while the electron remains localized in the bottom dot. The tunneling of holes creates molecular states that are the symmetric and antisymmetric combinations of the two basis states where the hole is in one dot or the other [9]. In analogy to real molecules, we call the symmetric (nodeless) molecular state, which has an enhanced wave function amplitude in the barrier, a bonding state. The antisymmetric (noded) state has a suppressed amplitude in the barrier and is called the antibonding state. These molecular orbitals are depicted schematically by the right-hand insets in Fig. 1. Intuitively one expects the molecular ground state to have bonding orbital character and the first excited molecular state to have antibonding orbital character.

The formation of molecular orbitals at an anticrossing is described by a simple Hamiltonian using an atomlike

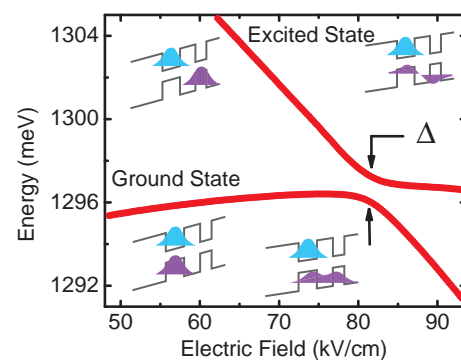


FIG. 1 (color online). Photoluminescence (PL) measurement of the electric field-induced anticrossing of X^0 at zero magnetic field for a sample with 2 nm barrier. Δ indicates the anticrossing energy gap. Insets: If the hole energy levels are out of resonance (left) the hole is localized in one of the individual dots. When the hole levels are tuned into resonance by the applied electric field, coherent tunneling leads to the formation of bonding (bottom right) and antibonding (upper right) molecular wave functions.

Report Documentation Page				Form Approved OMB No. 0704-0188	
Public reporting burden for the collection of information is estimated to average 1 hour per response, including the time for reviewing instructions, searching existing data sources, gathering and maintaining the data needed, and completing and reviewing the collection of information. Send comments regarding this burden estimate or any other aspect of this collection of information, including suggestions for reducing this burden, to Washington Headquarters Services, Directorate for Information Operations and Reports, 1215 Jefferson Davis Highway, Suite 1204, Arlington VA 22202-4302. Respondents should be aware that notwithstanding any other provision of law, no person shall be subject to a penalty for failing to comply with a collection of information if it does not display a currently valid OMB control number.					
1. REPORT DATE SEP 2008		2. REPORT TYPE		3. DATES COVERED 00-00-2008 to 00-00-2008	
4. TITLE AND SUBTITLE Antibonding Ground States in InAs Quantum-Dot Molecules				5a. CONTRACT NUMBER	
				5b. GRANT NUMBER	
				5c. PROGRAM ELEMENT NUMBER	
6. AUTHOR(S)				5d. PROJECT NUMBER	
				5e. TASK NUMBER	
				5f. WORK UNIT NUMBER	
7. PERFORMING ORGANIZATION NAME(S) AND ADDRESS(ES) Naval Research Laboratory, 4555 Overlook Avenue SW, Washington, DC, 20375				8. PERFORMING ORGANIZATION REPORT NUMBER	
9. SPONSORING/MONITORING AGENCY NAME(S) AND ADDRESS(ES)				10. SPONSOR/MONITOR'S ACRONYM(S)	
				11. SPONSOR/MONITOR'S REPORT NUMBER(S)	
12. DISTRIBUTION/AVAILABILITY STATEMENT Approved for public release; distribution unlimited					
13. SUPPLEMENTARY NOTES					
14. ABSTRACT					
15. SUBJECT TERMS					
16. SECURITY CLASSIFICATION OF:			17. LIMITATION OF ABSTRACT Same as Report (SAR)	18. NUMBER OF PAGES 4	19a. NAME OF RESPONSIBLE PERSON
a. REPORT unclassified	b. ABSTRACT unclassified	c. THIS PAGE unclassified			

basis with a hole either in one dot or the other:

$$\hat{H} = \begin{pmatrix} E_0 & -t \\ -t & E_0 - f + f_0 \end{pmatrix}. \quad (1)$$

Here E_0 is the energy of the localized hole states at resonance, t is the tunneling rate, and $f = e\tilde{d}F$ is the Stark energy due to the electric field F . The energies of the bonding and antibonding molecular orbitals are given by the eigenvalues of Eq. (1). When the electric field is tuned to resonance ($f = f_0$), the energies are $E_b = E_0 - t$ and $E_{ab} = E_0 + t$. The magnitude of t is determined by the splitting between the two molecular states: $2t = E_{ab} - E_b$. The sign of t is determined by which orbital state is at higher energy. However, the sign of t cannot be measured from anticrossing energy gaps ($\Delta = 2|t|$) in photoluminescence (PL) spectra like that of Fig. 1.

Using magneto-PL we can directly measure the orbital character of the molecular states and determine the sign of t [10]. When a magnetic field is applied to InAs/GaAs QDMs with a 2 nm GaAs barrier there is a large resonant change in the Zeeman energy splitting as a function of electric field [10]. This effect is shown in Fig. 2(a), where we plot the PL lines of the same QDM shown in Fig. 1, but now in a longitudinal magnetic field of $B = 6$ T. The resonant change in Zeeman splitting is plotted in Fig. 2(c). The black [gray (red)] shading indicates the resonant change in Zeeman splitting for the molecular ground (excited) state. As discussed below, the resonant changes in

Zeeman splitting arise from the contribution of the GaAs barrier to the net g factor for the delocalized hole [10].

In Figs. 2(d)–2(f) we show the measured change in Zeeman splitting from samples with increasing barrier thickness d . When $d = 3$ and 4 nm [Figs. 2(d) and 2(e)], there is a dramatic *reversal* in the nature of the resonance: the molecular ground state (black shading) now shows a resonant *increase* in Zeeman splitting and the first molecular excited state [gray (red) shading] now shows the resonant *decrease* in Zeeman splitting. The amplitude of the resonant change in Zeeman splitting decreases as the thickness of the barrier increases, and is below our noise level for $d = 6$ nm [Fig. 2(f)]. The decreasing amplitude results from the reduction of the amplitude of the wave function in the barrier with increasing barrier thickness. We will first show from an analysis of the data that the inversion of the Zeeman resonance can be understood as a change in the sign of t . Then we will discuss how this can be understood from theoretical considerations.

To quantitatively analyze the resonant changes in Zeeman splitting (Fig. 2) and the associated tunneling rates, we add the Zeeman interaction to Eq. (1):

$$\hat{H}_{\uparrow\downarrow(\downarrow\uparrow)} = \begin{pmatrix} E_0 \mp h_0 & -t \mp h' \\ -t \mp h' & E_0 \mp h_0 - f + f_0 \end{pmatrix}. \quad (2)$$

We obtain two Hamiltonians for the two spin configurations $\uparrow\downarrow$ and $\downarrow\uparrow$, where (\uparrow, \downarrow) and (\downarrow, \uparrow) are the electron spin and hole spinor projections, respectively. The diagonal part, $h_0 = (g_e + g_h)\mu_B B/2$, is just the normal Zeeman energy for the isolated dots. g_e and g_h are the g factors for electrons and holes. The off-diagonal part, h' , creates a spin-dependent contribution to the tunneling rate ($-t \Rightarrow -t \pm h'$), which is responsible for the resonant change in Zeeman splitting [11].

To obtain an expression for the Zeeman splitting of the ground (Δ_G) and excited (Δ_E) states, we take the difference between the eigenvalues for the two spin states in Eq. (2):

$$\Delta_{G(E)} = \left| 2h_0 \pm \frac{4th'}{\sqrt{(f - f_0)^2 + 4t^2}} \right|. \quad (3)$$

Using Eq. (3) we obtain the fits to the Zeeman resonance data shown in Figs. 2(c)–2(f). The off-resonant value of the splitting is determined by h_0 and the magnitude of the resonance is given by h' . The fit values are given in the figure caption. The width of the resonance is determined by the magnitude of the tunneling rate t , which is independently determined by the anticrossing energy (for example, Δ in Fig. 1).

This analysis leads to a simple intuitive description of the origin of the resonant change in Zeeman splitting. As the electric field tunes the states of the two dots into resonance, the formation of molecular orbitals with bonding or antibonding character changes the amplitude of the molecular hole wave function in the barrier, which has a different hole g factor [10]. The second term on the right-

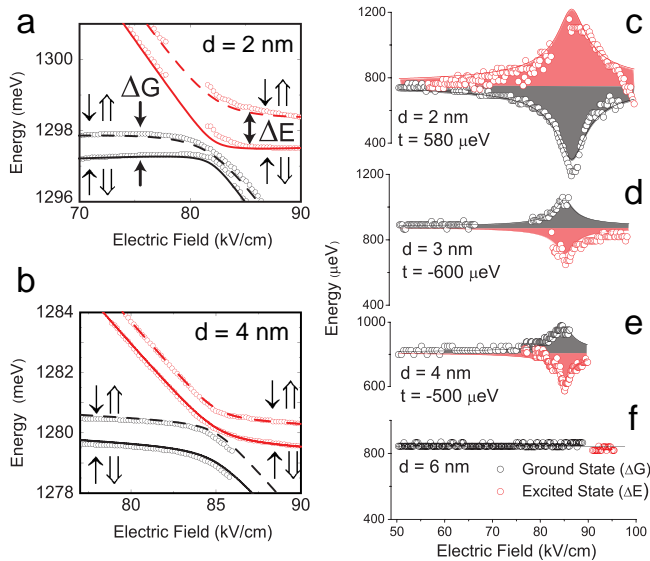


FIG. 2 (color online). Zeeman energy splitting as a function of applied electric field for $B = 6$ T. (a),(b) Energies of the X^0 PL lines for QDMs with 2 and 4 nm barriers. Solid lines and dashed lines calculated using Eq. (2) indicate the two separate spin configurations. (c)–(f) QDMs have a barrier thickness of (c) 2, (d) 3, (e) 4, and (f) 6 nm. Solid curves are calculated with Eq. (3) using $(h_0, h') = (-0.368, 0.229), (-0.446, 0.082), (-0.404, 0.076)$ meV for 2, 3, and 4 nm, respectively.

hand side of Eq. (3) captures the resonant change in the contribution from the barrier (h') and is responsible for the resonant change in the Zeeman splitting. The relative signs of the first and second terms in Eq. (3) determine whether there is a resonant enhancement or suppression of the splitting. We find that h_0 is negative [12]. Thus if $h't$ is positive, the Zeeman splitting of the ground state is suppressed at resonance and the splitting of the excited state is enhanced. This is what we measure for the $d = 2$ nm sample. We will show below from theory that $t > 0$ for thin barriers, corresponding to the normal case where the ground state is a bonding orbital. Therefore h' is also positive.

We make the assumption that the sign of h' does not change as the barrier thickness is increased. This assumption is reasonable: as the barrier becomes thicker, the sign of h' should tend toward the g factor for holes in bulk GaAs, which is known to be positive [13,14]. Because h' remains positive, it is a change of sign of t in Eq. (3) that leads to the inversion of the resonant Zeeman energy splitting as the barrier thickness is increased. This reversal in the sign of t means that there is a reversal of the energy of the bonding and antibonding states, i.e., the antibonding state becomes the energetic ground state. We now consider the theoretical origin of such a reversal and show that it is a result of the SO interaction.

Holes experience a strong SO interaction because they are derived from p -type atomic orbitals of the semiconductor lattice [15]. In QDMs, the SO interaction couples the hole's atomic orbital and spin degrees of freedom to give a total (Bloch) angular momentum $J = 3/2$. $J_z = \pm 3/2$ projections correspond to heavy holes and $J_z = \pm 1/2$ to light holes. Because the light-hole states are shifted up in energy by confinement and strain, it is often useful to represent the two low-energy (heavy-hole) states as pseudo-spin-1/2 particles (\downarrow, \uparrow). When the heavy-light-hole mixing is included, low-energy hole states can be described within the Luttinger-Kohn $k \cdot p$ Hamiltonian formalism as four component Luttinger spinors [3]. Each spinor is an admixture of all four projections of J_z , with the heavy hole typically the dominant component. However, as we show here, minor components of no more than 5% are sufficient to substantially alter the character of the molecular orbitals.

The influence of the minor components is apparent from Fig. 3. In Fig. 3(a), we plot the energies of the molecular ground and first excited states for asymmetric QDMs subject to a resonant electric field calculated using a simple one-band effective mass model, which neglects SO interactions. As expected, the energy separation of the bonding (solid black line) and antibonding (dashed red line) states decreases as a function of increasing barrier thickness and the bonding orbital remains the molecular ground state. In Fig. 3(b) we show the energies of the bonding (solid blue line) and antibonding (dashed red line) states calculated

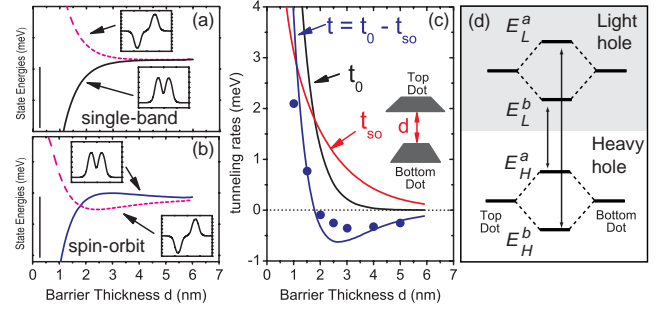


FIG. 3 (color online). (a),(b) Energy of the ground and first excited molecular states as a function of d calculated using (a) the single-band effective mass and (b) $k \cdot p$ theory. Scale bars are 5 meV. Insets show the orbital character of the dominant hole spinor component. (c) Tunneling rates of a single hole versus d calculated as described in the text. Inset: Schematic depiction of a QDM. (d) Schematic depiction of the SO induced mixing between bonding (E^b) and antibonding (E^a) molecular states of the heavy (E_H) and light (E_L) holes.

using a four-band $k \cdot p$ model that includes the SO interaction. At $d \sim 1.75$ nm the energies of the bonding and antibonding states cross and the antibonding state becomes the molecular ground state. We estimate the antibonding character of the ground state spinor for large barrier thicknesses to be as large as 95%, many times larger than in known atomic systems [16].

In Fig. 3(c) we plot the values for t_0 and t , i.e., half the difference between the state energies given in Figs. 3(a) and 3(b), respectively. In the absence of SO interaction, the tunneling rate is determined simply by the overlap between the hole orbitals of the individual dots (t_0), which decreases exponentially with increasing barrier thickness at a rate dependent on the heavy-hole mass. When the SO interaction is included, there is a correction to the tunneling rate, $t = t_0 - t_{so}$. This t_{so} term arises from the small contribution of the light-hole component of the spinor. The light-hole component has approximate parity along z opposite to that of the heavy-hole component [3,16]. The light-hole component therefore adds a small antibonding (bonding) component to the bonding (antibonding) state determined by the dominant heavy-hole component, as shown schematically in Fig. 3(d). The addition of this antibonding component increases the energy of the bonding state and vice versa for the antibonding state. As the barrier thickness increases, t_{so} does not decrease as fast as t_0 , in part because of its light-hole origin. For thin barriers, the t_{so} correction is small compared to the large t_0 , and t remains positive. However, for thicker barriers t_0 decreases and becomes comparable to t_{so} . When $t_0 < t_{so}$ the tunneling rate is negative and the antibonding orbital is the molecular ground state.

We have verified that this simple four-band $k \cdot p$ approach captures the essential physics of the system by comparison with an atomistic calculation (using $>10^6$

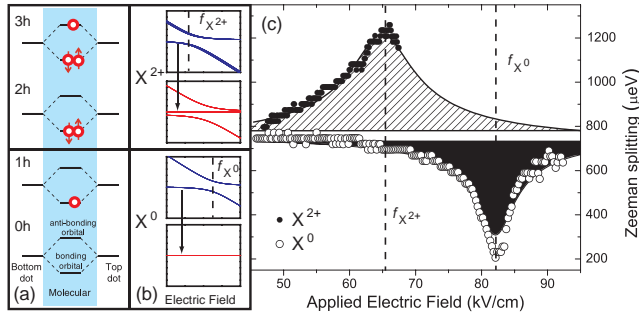


FIG. 4 (color online). (a) Molecular ground states for each charge configuration are determined by sequentially filling molecular orbitals with holes. (b) Calculated energy levels for the X^{2+} transition (from three holes plus one electron to two holes) and the X^0 transition (from one hole plus one electron to zero holes). (c) Electric field dependence of the Zeeman splitting for the X^0 and X^{2+} molecular ground states in a QDM with 2 nm barrier at $B = 6$ T. The resonances peak at two different values of the electric field (f_{X^0} and $f_{X^{2+}}$) because of different Coulomb interactions.

atoms) of the hole levels of a QDM described by the $sp^3d^5s^*$ tight-binding model [16]. This approach accounts for strain and changes to the underlying crystal lattice on the atomistic level. The results of this calculation [solid blue points in Fig. 3(c)] qualitatively match the $k \cdot p$ results.

Our theoretical model predicts an antibonding molecular ground state for a barrier thickness $d \geq 1.75$ nm. Experimentally, we find that all examples (7) in the sample with $d = 2$ nm have a molecular ground state with bonding orbital character; in the sample with $d = 4$ nm, all examples (3) have an antibonding ground state. The intermediate case ($d = 3$ nm) has examples of both types of behavior, indicating that the reversal of orbital character occurs near $d = 3$ nm. The small discrepancy with theory most likely arises from details of dot structure, and the coexistence of both behaviors at $d = 3$ nm most likely arises from fluctuations.

We now consider what happens when we add additional holes to the molecular orbitals. In Fig. 4(a) we schematically depict the filling of the molecular orbitals when the bonding state is the lowest energy single particle state (i.e., $d = 2$ nm). The lowest energy two-hole state is a spin singlet with bonding character that has no magnetic field spin splitting. The lowest energy three-hole state must have an unpaired hole in the antibonding orbital. Because of the unpaired hole, this state should have a magnetic field splitting like that of the one-hole state, but the Zeeman splitting should increase on resonance because the unpaired hole is in the antibonding orbital. This is exactly what we observe, as shown in Fig. 4(c). The one-hole and three-hole states of the same QDM (with $d = 2$ nm) have opposite behavior, indicating that they have different orbi-

tal character. The three-hole state is observed as the initial state of the doubly charged exciton (three holes and one electron) [16,17].

Here we have presented the first experimental observation of an antibonding molecular ground state. Antibonding molecular ground states are never observed in natural molecules, so this result provides a striking example of the new properties that can be engineered using semiconductor nanostructures. Our result specifically demonstrates that the SO interaction can be used to design hole molecular ground states with arbitrary orbital character. Possible applications in spintronics and quantum information processing include designing structures and protocols to coherently control single confined spins with electric fields or g tensor modulation [18].

We acknowledge support from NSA/ARO, ONR, CIAR, QuantumWorks, FIRB-MIUR Italy-Canada RBIN06JB4C, MEIF-CT-2006-023797 (J. I. C.), and Institute for Microstructural Sciences (J. I. C.).

*doty@udel.edu

Present address: Department of Materials Science and Engineering, University of Delaware, Newark, DE 19711, USA.

- [1] G. Bester, A. Zunger, and J. Shumway, Phys. Rev. B **71**, 075325 (2005).
- [2] W. Jaskolski *et al.*, Phys. Rev. B **74**, 195339 (2006).
- [3] J. I. Climente, M. Korkusinski, and P. Hawrylak, Phys. Rev. B **78**, 115323 (2008).
- [4] M. Bayer *et al.*, Science **291**, 451 (2001).
- [5] H. J. Krenner *et al.*, Phys. Rev. Lett. **94**, 057402 (2005).
- [6] G. Ortner *et al.*, Phys. Rev. Lett. **94**, 157401 (2005).
- [7] E. A. Stinaff *et al.*, Science **311**, 636 (2006).
- [8] A. S. Bracker *et al.*, Appl. Phys. Lett. **89**, 233110 (2006).
- [9] G. Schedelbeck *et al.*, Science **278**, 1792 (1997).
- [10] M. F. Doty *et al.*, Phys. Rev. Lett. **97**, 197202 (2006).
- [11] The potential barrier height is effectively increased or decreased by the maximum barrier contribution to the Zeeman energy h' . As can be seen in Fig. 2(a) this term leads to an enhanced (dashed lines) or suppressed (solid lines) anticrossing energy for the two values of the hole spin.
- [12] For example, using magneto-PL at varying angles of the magnetic field we find $g_e = -0.745$ and $g_h = -1.4$ in the sample with $d = 2$ nm. This is consistent with a previous study of single InAs dots. M. Bayer *et al.*, Phys. Rev. B **61**, 7273 (2000).
- [13] V. A. Karasyuk *et al.*, Phys. Rev. B **49**, 16381 (1994).
- [14] M. J. Snelling *et al.*, Phys. Rev. B **45**, 3922 (1992).
- [15] J. M. Luttinger and W. Kohn, Phys. Rev. **97**, 869 (1955).
- [16] See EPAPS Document No. E-PRLTAO-102-044906 for additional information. For more information on EPAPS, see <http://www.aip.org/pubservs/epaps.html>.
- [17] M. F. Doty *et al.*, Phys. Rev. B **78**, 115316 (2008).
- [18] Y. Kato *et al.*, Science **299**, 1201 (2003).